

DOI: 10.1515/amm-2016-0190

M. STEGLIŃSKI^{*,#}, P. BYCZKOWSKA^{*}, J. SAWICKI^{*}, Ł. KACZMAREK^{*}, B. JANUSZEWICZ^{*}, M. KLICH^{*}**SYNERGY OF THE PLASTIC TREATMENT HPT AND SHOT PEENING IN ALUMINIUM ALLOY Al-Mg-Mn-Sc-Zr**

An improvement in fatigue strength is one of the main factors enabling the use of high-durability Al-Mg-Mn-Sc-Zr alloys in functional components of mobile robots. As part of this study, a computer simulation was carried out using ANSYS LS-DYNA software that involved the hybridization of high pressure torsion (HPT) and shot peening (SP) forming processes. The numerical analysis was aimed at determining residual stresses and strains that affect the durability and stress characteristics of the analyzed Al alloy. Results of the study indicate that tensile stresses of $\sigma = 300$ MPa generated as a result of HPT are transformed into a beneficial stress of $\sigma = 25$ MPa resulting from plastic strains caused by SP surface treatment.

Keywords: high-pressure torsion, shot peening, numerical analyses, residual stresses, fatigue strength

1. Introduction

The rapidly developing field of non-stationary robotics (e.g. UAVs, drones, rovers) is aiming to improve reliability and functionality. Attempts are made to develop the robots' functionality by increasing their operating time, which is achieved directly through increasing battery capacity or indirectly through decreasing the robots' mass. Reduction of mass can be attained through modifying the robots' propulsion system, which are usually constructed from medium quality alloy steel or titanium alloys. These materials could be replaced by aluminum alloys, characterized by a lower density and comparable fatigue limit specifications. The durability requirements set for functional elements could be met by series 2xxx, 7xxx and 8xxx aluminum alloys, but these alloys are disqualified from these applications due to their level of resistance to contact fatigue.

Improvement of fatigue limit characteristics of every material can be achieved through selective heat treatment or plastic strain that generates compressive stress in near-surface areas. The 5xxx series of aluminum alloys is intended for heat treatment, however, a lack of alloy additions that allow for precipitation hardening means that these alloys do not achieve high mechanical parameters. A study carried out by Zaki A., Anwar U. and Costa S. and all, proves that doping 0.25% Sc into Al-Mg alloys causes an increase in durability to 375 MPa while maintaining an elongation of $A = 29\%$ [1, 2]. The increase in durability, connected with intermetallic precipitates in Al₃Sc, is achieved thanks to a high dispersion and density of phases. Furthermore, studies carried out by Jia Z., Røyset J [3], prove that a simultaneous addition of Sc and Zr causes the creation of an Al₃Zr_x phase which

is metastable with an isomorphous precipitation of Al₃Sc. Adding Sc and Zr elements, characterized by different diffusion ratios, and carrying out selective heat treatment in Al-Mg alloys means that precipitates can be created, made up of a core (Al₃Sc) and a surrounding shell of Zr, described as Al₃(Sc_xZr_{1-x}) [3]. Optimization of the chemical composition of an Al alloy containing 5% Mg, carried out by Kun Y., Wenxian L. and other researchers [4], proved that an addition of 0.6% Sc and 0.1% Zr allowed the material to achieve the best mechanical parameters and the highest fragmentation of structure. According to studies carried out by Christian B. Fuller [5], the most beneficial percentage ratio of Sc to Zr to be adopted when attempting to increase the performance characteristics of Al alloys is (Sc):1(Zr). Research into Al-Mg-Mn alloys indicates [5] that aside from increasing durability, adding Sc and Zr also affects the alloy's recovery and recrystallization, upping the recrystallization temperature to 600°C, which positively impacts the ability to perform forming processes with significant deformation [4].

Forming processes cause the strengthening of material through generating specific stresses inside. Depending on their character, stresses can increase or decrease certain parameters of the material. Depending on the area of stresses introduced into the material, forming processes can be divided into extrusion and surface processes. Extrusion processes include SPD (Severe Plastic Deformation) techniques, i.e. ECAP (Equal-Channel Angular Pressing), HPT (High-Pressure Torsion) and TE (Twist Extrusion), while surface processes include SP (Shot Peening).

According to studies carried out by Meguid S.A., Shagal G., performing the HPT process causes plastic strains to occur in the Al alloy, which results in the fragmentation of the material's

* LODZ UNIVERSITY OF TECHNOLOGY, INSTITUTE OF MATERIALS SCIENCE AND ENGINEERING, 1/15 STEFANOWSKIEGO STR., 90-924 LODZ, POLAND

Corresponding author: mariusz.steglinski@p.lodz.pl

structure to grain size = 70 nm and in a change in the state of stresses [5]. Change in the state of stresses versus strain occurs in the areas located above the circle inscribed in the cross section of the treated material. Depending on the crystallographic orientation, process forming using the HPT method will generate compressive or tensile stress [5]. According to research carried out by Li J., Peng Z., the generated stresses and fragmentation of structure causes an improvement in durability parameters [7]. However, the same research shows that the distribution of stresses is not balanced or unidirectional. As a result of HPT treatment, compressive stresses are generated in the axial area, but as the radius of distance from the stress axis increases, negative stresses decrease and become positive near the surface [6-9].

According to studies carried out by H-Gangaraj S.M. and Alvandi-Tabrizi Y., fatigue limit depends on the type of stresses present in the materials. Compressive stresses are the most beneficial stresses which increase the fatigue limit of the surface stratum [10].

Studies carried out by [11-15] indicate that the SP process generates compressive stresses. Research carried out by Benedetti M., Fontanari V. using alloy AA7050-T7451 has shown that the diameter of shot used does not significantly affect the amount of residual stresses. It does however significantly influence the range of generated stress [11]. Aside from the above-mentioned factors, the range of stresses generated during the process depends on the working pressure, distance between the nozzle and the angle of attack of the processing medium. C.A. Rodopoulos and A. Ebenau [12] have confirmed that the range of generated stresses increases with working pressure. However, above a certain limit of pressure the range of maximum stresses is lowered. Another parameter, the distance between the nozzle and the processed material, is inversely proportional to the range of generated stresses. This dependence is constant for all distances between the nozzle and the object. As in the case of pressure, the impact of the angle of attack of the processing material on the range of stresses is variable. Research carried out by Jianming W., Feihong L. and Meguid S.A. indicates that cyclical stress of 300 MPa results an over 10-fold increase of the fatigue limit in comparison to other conventional process forming techniques that generate compressive stress [13-15].

Hybridization of SPD processing has so far received a marginal treatment in literature available on the subject. This study will analyze a hybridization of HPT and SP treatment in order to generate compressive stresses on the surface of an aluminum alloy that had previously undergone extrusion treatment.

2. Definition of the numerical model

The study was carried out using ANSYS LS-Dyna software. The geometrical model was created using SOLID EDGE ST4 software and comprised four components. First and second component of model was the HPT matrix. The next component consisted of the analyzed sample, measuring $\varnothing 25 \times 5$ mm. The matrix component was modelled as non-deformable.

In order to determine the material parameters of the analyzed material, the Johnson-Cook plasticity model was used, as well as isotropic elasticity in the values specified in table 1. The last component of the model consisted of three shot pellets measuring $d = 1.0$ mm, placed at a length of 70 mm from the processed surface. Both the shot pellet material and the matrix were modelled as non-deformable.

TABLE 1
Mechanical properties of materials used in analysis

Material	Modulus of Elasticity [MPa]	Poissons Ratio	Density [kg/m ³]	Tensile Strength, Yield [MPa]	Tensile Strength, Ultimate [MPa]
Al-Mg-Mn-Sc-Zr	71 000	0,33	2 650	575	625

The geometric model was discretised and was composed of 19 208 components and 19 867 nodes, taking into account the densifying on working edges and a maximum size of finite elements in the analyzed sample of 1 mm.

The numerical analysis of the hybrid HPT and SP process comprised two stages. The first stage consisted of performing an extrusion HPT forming process. The numerical analysis of the HPT process involved an interaction in the form of slide-separation with a friction coefficient of 0.5. The pressure (4 000 MPa) was load to the upper component of matrix. The upper component of matrix was rotated by 90 degree. The second stage of the analysis involved blasting shot pellets at external surfaces of the previously strained sample. As part of the second stage, an interaction of slide-separation without friction was set up. The pellets were set into motion by a force of 0.6 MPa perpendicular to the treated surface (Fig. 1).

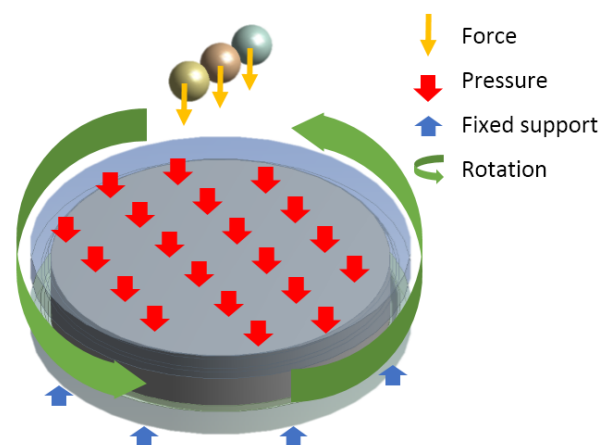


Fig. 1. Discrete model of the hybrid process of HPT and SP numerical analysis

3. Results

The area in which results were observed constituted a circle with a diameter of 25 mm. Areas of technological deformation were left out due to their later removal through material removal

processing. The results of numerical analysis of the HPT process confirm that the research sample is deformed in its entirety during its compression and turn (Fig. 2a). As a result of the deformation, the height of the sample is decreased by over 50%. The fact that the sample is turned at the same time as it is compressed means that the distribution of deformations is not uniform across the analysed sample. The largest deformations, $\epsilon = 0.89$ mm, appear near the side edges of the processed sample. The numerical analysis also indicates that the center of the sample undergoes

the smallest deformation $\epsilon = 0.2$ mm. The intense plastic strains are accompanied by the generation of stresses (Fig. 2b-e). The maximum reduced stresses obtained through simulating the HPT process are present in the central area of the sample and amount to $\sigma = 400$ MPa (Fig. 2b). Analysis of normal stresses in the X, Y, Z directions (Fig. 2c-e) indicates that compressive stresses appear in the entire volume of the sample. The maximum value of compressive stresses appears in the lower central part of the sample (ca. 4 000 MPa) and decreases as distance from this point increases.

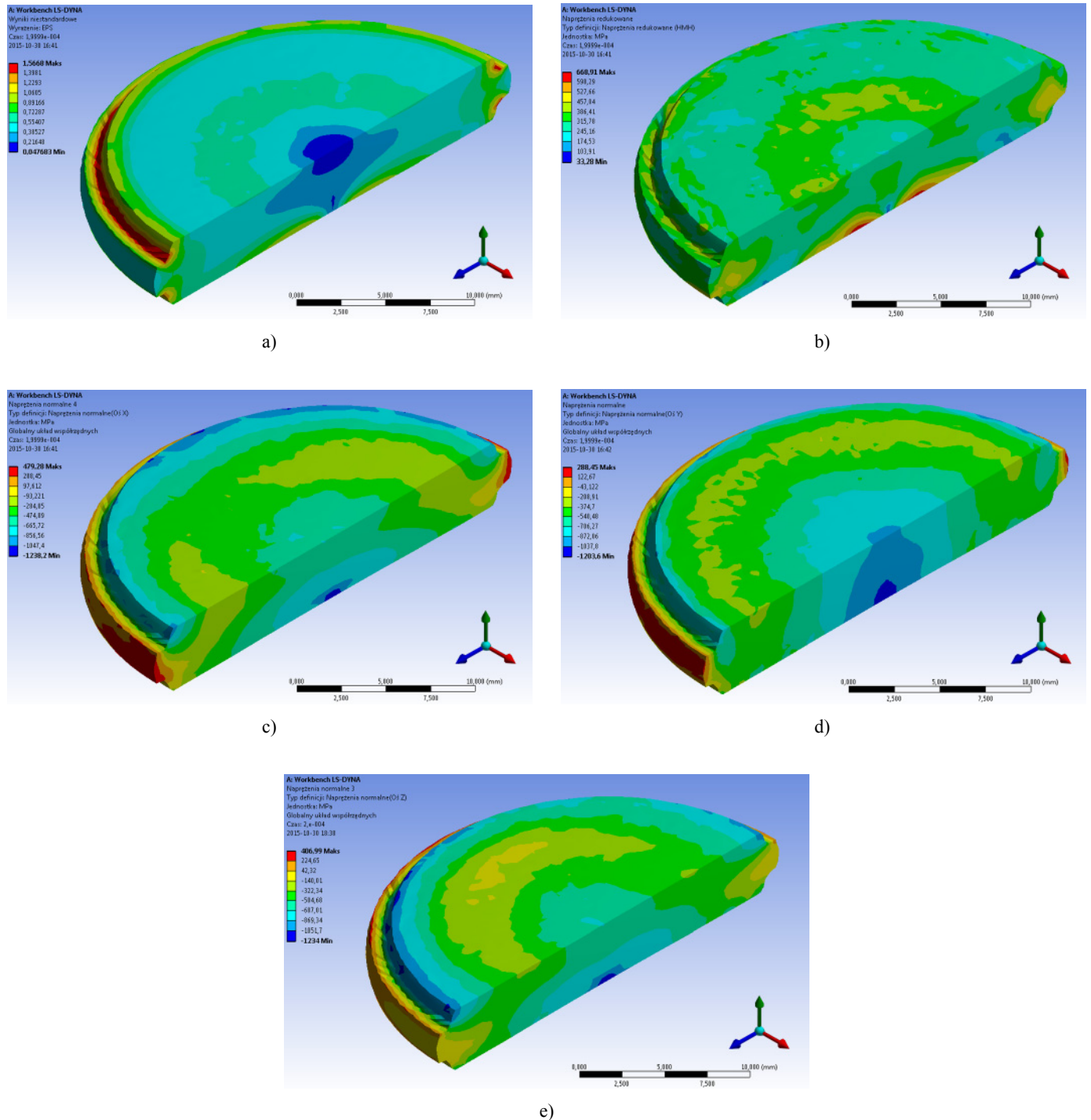


Fig. 2. Results of numerical simulation of the high-pressure torsion process, a) distribution of total strains, b) distribution of reduced stresses, c) distribution of normal stresses in X direction, d) distribution of normal stresses in Y direction, e) distribution of normal stresses in Z direction

Analysis of the results of the shot peening process indicates that the surface area is deformed only in the locations where it was impacted by pellets (Fig. 3a). The largest deformations can be found on the surface and amount to $\varepsilon = 0.13$ mm. Observations indicate that the deformations penetrate into the material ca. 2 mm deep. The maximum reduced stresses (Fig. 3b) obtained through this process amount to $\sigma = 125$ MPa and are located

on the surface, between impact locations. Analysis of the state of normal stresses in the X (Fig. 3c) and Y (Fig. 3d) directions indicates that both tensile stresses of a maximum strength of $\sigma = 74$ MPa and compressive stresses of a maximum strength of $\sigma = -134$ MPa appear in the area of the plastic deformation and its impact zone. The largest stresses are located ca. 0.75 mm deep under the surface.

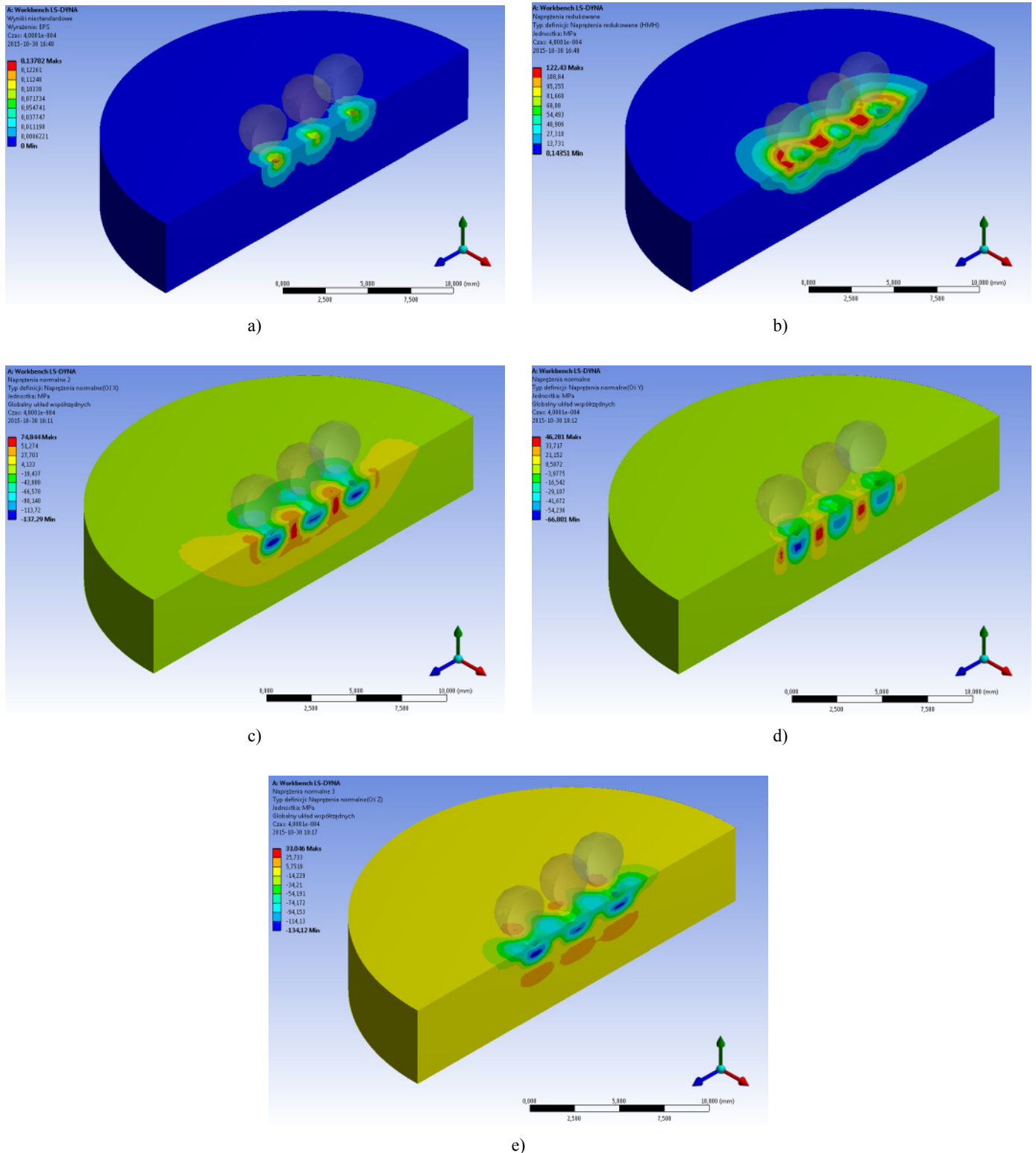


Fig. 3. Results of numerical simulation of the shot peening process, a) distribution of total strains, b) distribution of reduced stresses, c) distribution of normal stresses in X direction, d) distribution of normal stresses in Y direction, e) distribution of normal stresses in Z direction

A numerical analysis of the synergical HPT and SP process indicates that the impact of pellets on a pre-compressed and pre-twisted surface causes a synergy of plastic deformation to appear. As a result of the synergy of the analysed plastic forming processes, deformations increase from 0.4 to 0.75 mm (Fig. 4a) and the distribution and value of stresses increases. The pellet impact results in a decrease in reduced stresses in the central part of the sample, from 380 MPa (Fig. 2b) to 25 MPa

(Fig. 4b). The type of stresses changes in a small area ca. 2.5 mm under the upper surface. The distribution of normal stresses in the X direction indicates that the pellet impact causes an increase in compressive stresses from $\sigma = -665$ MPa (Fig. 2c) to $\sigma = -1\,350$ MPa (Fig. 4c). With regards to normal stresses in the Y direction (Fig. 4d), the compressive stresses increase mainly on the surface in the pellet impact zones, up to a value of $\sigma = -1\,390$ MPa.

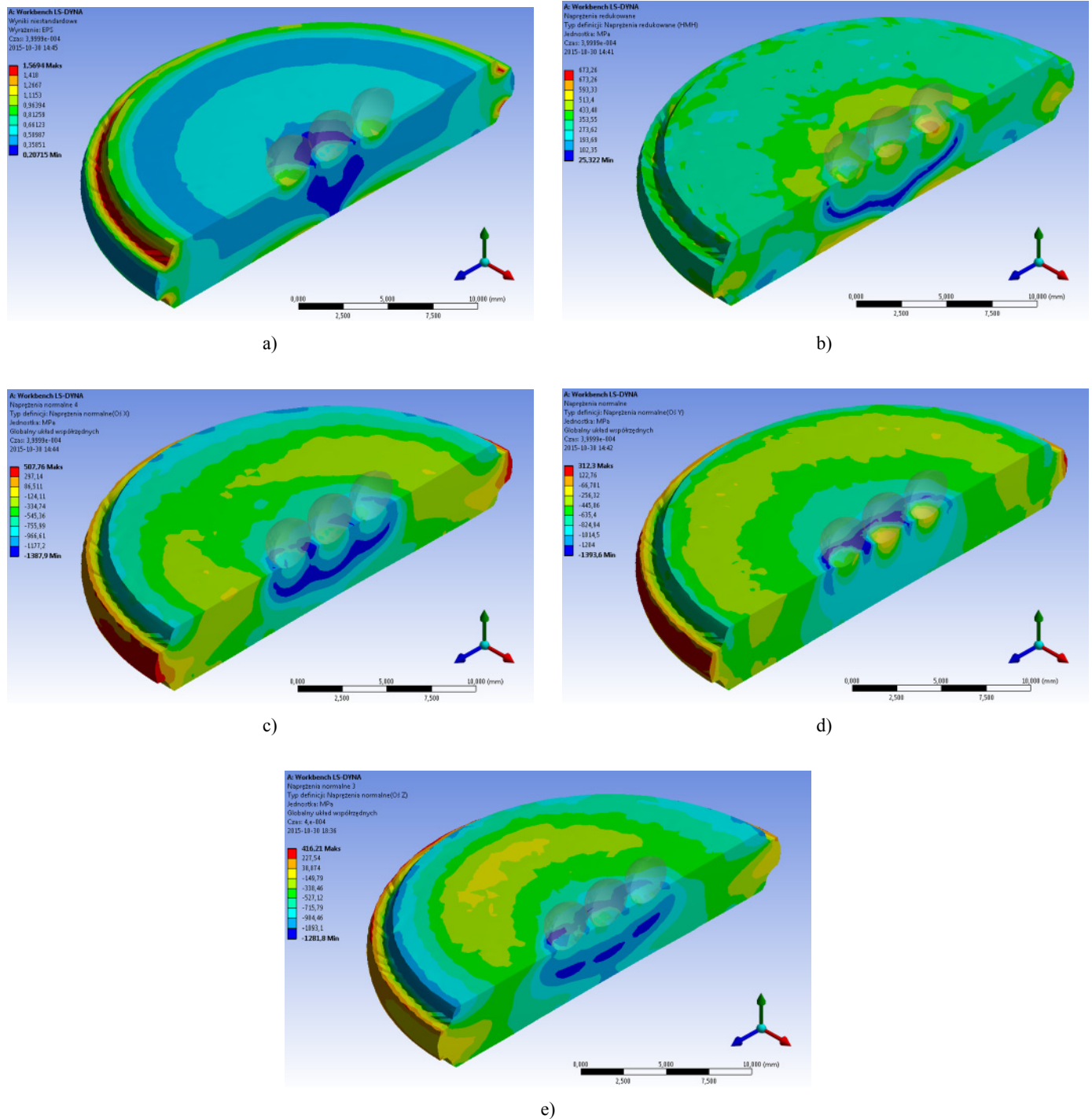


Fig. 4. Results of numerical simulation of the high-pressure torsion with shot peening process, a) distribution of total strains, b) distribution of reduced stresses, c) distribution of normal stresses in X direction, d) distribution of normal stresses in Y direction, e) distribution of normal stresses in Z direction.

4. Experimental verification

Numerical analysis of hybrid metal forming in shot-peening process and HPT has been verified against experiment results. As part of the experimental processes, the shot-peening process was conducted (sample of Al alloy $\varnothing 25 \times 5$ mm) at 0.6 MPa working pressure, 70 mm distance of the sample from the nozzle, and 90° tool rake angle. For the independent sample (sample of Al alloy $\varnothing 8 \times 2$ mm) only the process of HPT plastic deformation was conducted at the clamp pressure of 4 000 MPa, and rotation angle of 360° . Because of the topography of the sample surface after the HPT process it is not possible to conduct an experimental hybrid shot-peening process and HPT.

4.1. Experimental research methodology

The stresses were measured applying the X-ray method with the use of the PROTO iXRD diffractometer, where the stresses were analysed axially from the surface of the sample. Residual stress measurements were performed to the following parameters: a chromium anode x-ray tube, $K_{\alpha 1}$ radiation, tube voltage 20 kV, tube current 4 mA, Bragg angle $2\theta = 156.31^\circ$ (reflections from the 222 planes), oscillation in beta angle = 3° , LPA corrections, x-ray beam aperture of 2 mm and a vanadium $K\text{-}\beta$ filter. The profiles of the obtained diffraction peaks were approximated as a Cauchy function where 100% peak height was assumed. X-ray elastic constants provided in the software data-

base were used: $(1/2) S_2 = 18.56 e^{-6} [1/\text{MPa}]$ and $-S_1 = 4.79 e^{-6} [1/\text{MPa}]$. The stresses after the shot-peening process and HPT were measured at 3 points (1 – axis, 2 – 0.5 distance from the center to the edge of the sample; 3 – at the edge).

4.2. Experimental tests results

The experiment results were confronted with the results of the numerical analysis (Tab. 2).

TABLE 2

Comparison of stress distribution as a function of distance from the surface for the experiment and numerical analysis of the shot-peening process (experimental tests)

	Shot peening [MPa]			HPT [MPa]		
	125	250	400	1	2	3
Simulation	-328	-220	-170	-120.0	-102.5	-56.0
Experiment	-278	-256	-171	-60.5	-56.4	-12.6
Differents	50	36	1	59.5	46.1	43.4
AVG Differents	29			49.6		

Observation of the experiment results of the shot-peening process indicates that the maximum stress is -290 MPa and is located at a depth of approx. $150 \mu\text{m}$ (Fig. 5). The mean maximum discrepancy between the stress values was ± 29.0 MPa. The values of stress differences between points 1, 2, 3 did not exceed ± 8.5 MPa.

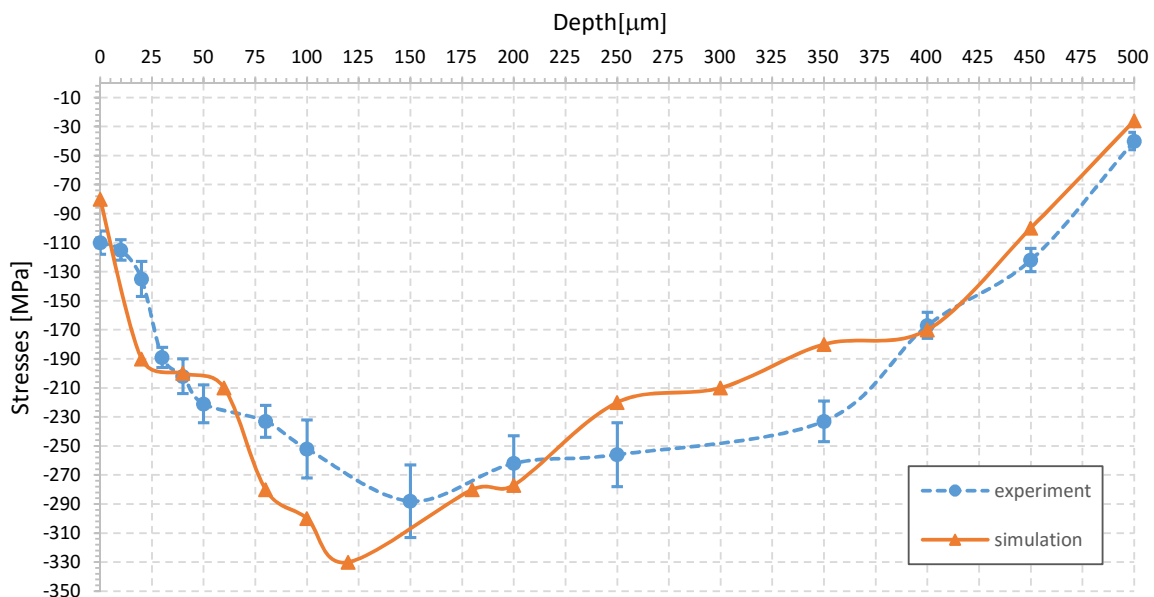


Fig. 5. Comparison of stress distribution as a function of distance from the surface for the experiment and numerical analysis of the shot-peening process (experimental tests)

The results of stress measurements after the HPT process (Fig. 6) indicate a variable stress distribution as a function of the measurement points on the sample surface (1 – axis, 2 – 0.5 distance from the center to the edge of the sample; 3 at the edge). The maximum stress values approx. -60.5 MPa were found at the

edge of the sample – and declined towards the center of the sample (-56.4 MPa for 0.5 distance from the center and -12.6 MPa at the center). The discrepancies between the results of the experimental and numerical analyses approximate 49 MPa both at the edge (59 MPa) and in the center of the sample (43 MPa).

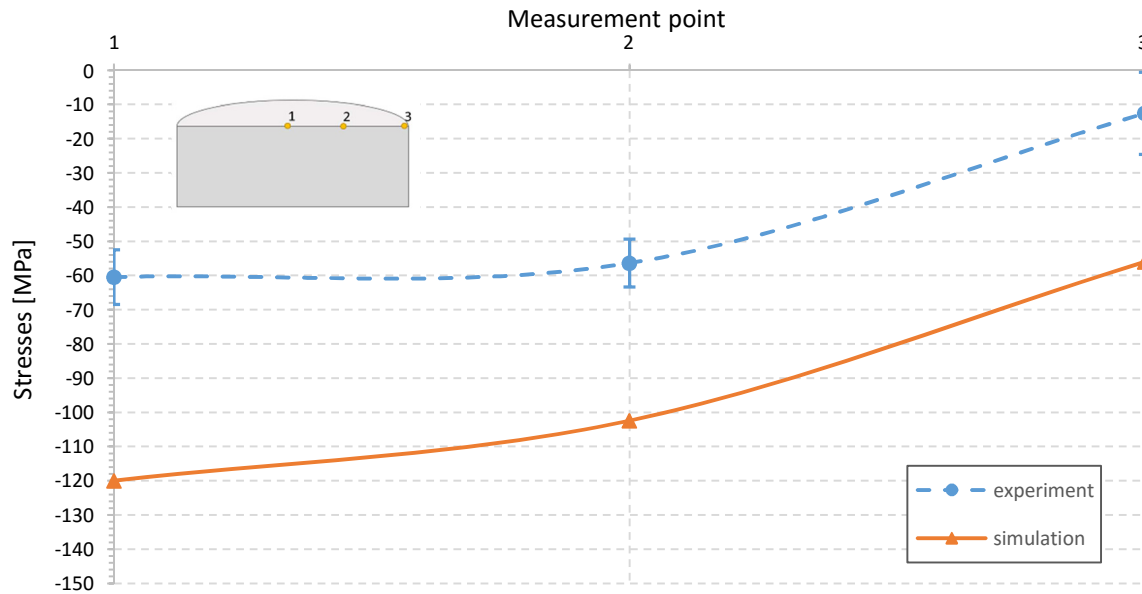


Fig. 6. Comparison of stress distribution for the relevant measurement points in experimental tests and the corresponding values of HPT numerical analysis

4.3. Summary of experimental tests

The experimental tests of the shot-peening process confirmed the results obtained from the numerical analysis, which cannot be directly concluded for the HPT process. However, given that the stress distribution for experimental and numerical tests in the HPT process is almost identical, it can be assumed that stress relaxation occurred as a result of dynamic, post-dynamic recrystallization during or after the process [16-17].

5. Summary

The performed numerical analyses indicated that the impact of shot pellets into the surface of a pre-twisted and pre-compressed sample causes a decrease in reduced stresses in the central area of the analysed material. Decrease in the reduced stresses results from the introduction of compressive stresses into the sub-surface area. Reduced stresses are decreased from $\sigma = 300$ MPa to $\sigma = 25$ MPa, which constitutes an over 10-fold decrease. The largest change of reduced stresses occurs ca. 2.5 deep under the surface, which in correlation with the range of plastic deformations caused by the shot peening process (c.a. 1.5 mm) indicates a wide range of effect of these deformations on the material. An analysis of normal stresses in the X and Y directions indicates that the change in the stresses does not constitute a simple sum of values from separate samples. The initial strengthening of the material due to the HPT process means that the impact of shot pellets into the surfaces of the sample causes more beneficial changes to stresses in locations adjacent to locations of maximum stresses than in the case of solely using the shot peening process. The beneficial changes in the distribution of normal stresses (from tensile to compressive) in a non-processed material following shot peening processing appeared in a transverse direction, while in

the material processed using the HPT process the changes appeared in a longitudinal direction. This indicates a change in the direction of strengthening due to pre-existing stresses.

The change in the distributions of stresses across the sample following the hybridisation of HPT and SP forming processes indicates a beneficial relaxation of stresses in the sample core (an increased elasticity of the core) with an increased strengthening of the surface (increase in compressive stresses within the range of effect of the SP sample). The obtained distribution of stresses secures the mating surfaces from the creation and propagation of microfractures. Such a distribution of stresses protects in the long term the mating surfaces of elements from the creation of nuclei of catastrophic fatigue fractures.

The performed computer analyses allow for estimating the range of appearance of unacceptable tensile stresses. We can therefore predict a high durability of the friction hub, both from the point of view of contact fatigue and fatigue durability, e.g. in meshing gears.

6. Conclusions

The performed analyses allowed us to prove the following statements:

- Hybridisation of HPT and SP processes causes the synergy of these forming processes to be more effective than the simple sum of their separate effects.
- The significant plastic deformation caused as a result of the HPT process means that the impact of the pellets on the surface of the sample cause an increase in the value of compressive stresses in the central part of the sample and their homogenisation.
- By combining the above processes, we were able to observe a change in the distribution of reduced stresses to a more

beneficial value from the point of view of durability parameters.

- The use of numerical methods in the process of optimising processes that use significant accumulation is much more cost effective in comparison to experimental research and allows for analysing both the distribution of stresses and strains, as well as for specifying potential locations where fracture nuclei will form.

Acknowledgments

This work was supported by the Polish State Committee for Scientific Research under project no. 2012/07/N/ST8/03099.

REFERENCES

- [1] A. Zaki, U. Anwar, *Corr. Sci.* **43**, 1227-1243 (2001).
- [2] S. Costa, H. Puga, J. Barbosa, A.M.P. Pinto, *Mat. Sci. and Design.* **42**, 347-352 (2012).
- [3] Z. Jia, J. Røyset, J. K. Solberg, Q. Liu, *Trans. Nonferrous Met. Soc. China* **22**, 1866-1871 (2012).
- [4] Y. Kun, L. Wenxian, L. Songrui, Z. Jun, *Mat. Sci. and Eng. A.* **368**, 88-93 (2004)
- [5] B. Fuller Christian, Submitted To The Graduate School In Partial Fulfillment Of The Requirements, Evanston, Illinois 2003.
- [6] S.A. Meguid, G. Shagal, J.C. Stranart, J. Daly, *Finite Elements in Analysis and Design.* **31**, 179-191 (1999).
- [7] J. Li, Z. Peng, C. Li, W. Chen, Z. Zheng, *Trans. Nonferrous Met. Soc. China* **18**, 755-762 (2008).
- [8] CN 103480789 – Pressure-torsion forming method of high-strength aluminium-alloy disc-shaped workpiece 2013.
- [9] CN 102189706- High-pressure shearing deformation method and device for tubular materials 2011.
- [10] S.M. H-Gangaraj, Y. Alvandi-Tabrizi, G.H. Farrahi, G.H. Majzobi, H. Ghadbeigi, *Trib. Inter.* **44**, 1583-1588 (2011).
- [11] M. Benedetti, V. Fontanari, P. Scardi, C.L.A. Ricardo, M. Bandini, *International Journal of Fatigue.* **31**, 1225-1236 (2009).
- [12] C.A. Rodopoulos, S.A. Curtis, E.R. de los Rios, J. Solis Romero, *International Journal of Fatigue.* **26**, 849-856 (2004).
- [13] S. Curtis, E.R. de los Rios, C.A. Rodopoulos, A. Levers, *International Journal of Fatigue.* **25**, 59-66 (2003).
- [14] W. Jianming, L. Feihong, Y. Feng, Z. Gang, *The International Journal of Advanced Manufacturing Technology* **56**, 571-578 (2011).
- [15] S.A. Meguid, G. Shagal, J.C. Stranart, *International Journal of Impact Engineering* **27**, 119-134 (2002).
- [16] R. Vafaei, M.R. Toroghinejad, R. Pippan, *Materials Science and Engineering A.* **536**, 73-81 (2012).
- [17] T. Sakai, A. Belyakov, R. Kaibyshev, H. Miura, J.J. Jonas, *Prog. Mater. Sci.* **60**, 130-207 (2014).